Numerical prediction of residual stresses induced by multi-pass GTA welding of martensitic steel X10CrMoVNb9-1

Guilhem Roux, René Billardon

Numerical prediction of residual stresses induced by multi-pass GTA welding of martensitic steel X10CrMoVNb9-1

Guilhem-Michel ROUX[1,2], **René Billardon**[2]

[2] *CEA (DEN/DANS/DM2S/SEMT/LM2S)*
[1] *LMT-Cachan*
61, avenue du Président Wilson, 94235 Cachan Cedex
roux@lmt.ens-cachan.fr

Abstract :

The nominal temperature in pressure vessels of future nuclear reactors -or so-called Very High Temperature Reactors using gas coolant at low pressure- should be around 450°C. Because of its microstructural stability at such a temperature, X10CrMoVNb9-1 martensitic steel -also known as ASTM A387 or T91 steel- is considered as a promising candidate material for these structures. Since, the manufacturing process of such thick pressure vessels will most probably involve GTA multi-pass welding, different studies are presently in progress in different laboratories to develop reliable tools for the failure assessment of multi-pass weld joints in structures made of X10CrMoVNb9-1 martensitic steel. The work presented herein is part of a study the aim of which is to develop finite element simulations of TIG multi-pass welding to predict the residual stresses induced by the process in the vicinity of welded joints in thick structures made of X10CrMoVNb9-1 martensitic steel. Since the accuracy of such complex thermo-metallo-mechanical finite element analyses strongly depends on many inputs, experiments have been designed to valide the numerical tool that is currently in development.

Résumé :

La température nominale de fonctionnement dans la cuve des futurs réacteurs nucléaires de type VHTR (Very High Temperature Reactors, utilisant comme fluide caloporteur un gaz) devrait être aux alentours de 450°C. La stabilité microstructurale à ces températures de l'acier martensitique X10CrMoVNb9-1(ASTM A387, également connu sous la dénomination commerciale "T91") en font un candidat pour ce type de structure. La fabrication de telles cuves de forte épaisseur fera vraisemblablement intervenir des opérations de soudage TIG multipasse . Plusieurs études sont actuellement en cours dans différents laboratoires afin de développer un outil prédictif de calcul de durée de vie des ces jonctions soudés soumises aux conditions de fonctionnement normales. Le travail présenté ici se focalise sur le développement d'outils numériques permettant de simuler un tel procédé afin de prédire les contraintes résiduelles induites. La performance de telles simulations, couplant à la fois thermique, métallurgie et mécanique, doit préalablement être validée dans des configurations simples.

Key-words :

thermo-metallo-mechanical simulations; martensitic-steel ; Satoh experiment

1 Introduction

Multi-pass welding process implies complex thermo-mechanical loading. At each pass, the material is heated from room temperature to much higher temperatures and then cooled down to room temperature. Temperature rates and maximum values of the temperature depend on the position of the considered point with respect to the arc weld. Moreover, in the case of thick -rigid- structures, these complex and highly non-uniform thermal loadings are coupled to non-negligible mechanical loadings. The residual stress state as well as the microstructure of the material after the process is fully dependent on these highly complex thermo-mechanical loading during the welding process. The objective of this study is to contribute to the development

in the finite element code Cast3M©-developed at CEA- of analyses coupling heat transfer, metallurgical transformation and mechanical models -using a sequential iterative procedure-.

2 Thermo-metallo-mechanical model

2.1 Heat transfer analyses

The heat transfer problem is solved by using a two-step θ method. Heat equation can be written as:

$$\rho C_p \frac{\partial T}{\partial t} - div\left[\lambda grad T\right] - \dot{D} + \dot{L} = 0 \tag{1}$$

where $\dot{L}$ and $\dot{D}$ respectively represent the latent heat that is associated to solid-solid or solid-liquid transformations and the mechanical dissipation. During GTA welding process it can be assumed that mechanical dissipation is negligible compared to other heat sources. During the process the microstructure of the material and hence the macroscopic thermal parameters ρC_p and λ strongly vary. To take account of the evolution of these macroscopic thermal parameters during out of equilibrium phase transformations -that are induced by high temperature rates, both during cooling and heating-, as a first approximation, the material can be considered as a collection of different phases so that these parameters can be derived from standard mixture laws:

$$\rho C_p = \sum_{i=1}^{n} \rho_i C_{p_i} \tag{2}$$

$$\lambda = \frac{1}{\sum_{i=1}^{n} \lambda_i} \tag{3}$$

where n represents the number of phases that are taken into account. The temperature evolution of the parameters must be identified for each phase from ad hoc experiments. Another key issue concerning heat transfer analyses concerns the boundary conditions, in other words the heat source that is representative of the GTA torch as well as the convection and radiation phenomena at every point at the surface of the welded parts. Different -surfacic or volumetric- heat source models have been proposed in the litterature and standard temperature evolution of so-called convection-radiation exchange parameter are available. However, specific simple well controlled experiments must be made to identify these boundary conditions (see for instance Roux *et al.* (2006)).

2.2 Metallurgical transformations

The microstructural stability of X10CrMoVNb9-1 steel is explained by its chemical composition and in particular the high percentage of chromium and the presence of vanadium and niobium (see 1).

The as-delivered microstructure of this material corresponds to tempered martensite. During heating, for instance during the welding process, depending on the maximum temperature reached, this base material may transform into austenite γ, ferrite δ or liquid. As a first approximation, the austenite to ferrite δ transformation can be ignored. During cooling, a martensitic transformation occurs for any cooling rate within the range that must be considered in practise.

composé	C	Si	Mn	P	S	Cr
wt%	0.086-0.12	0.20-0.50	0.30-0.60	max 0.02	max 0.01	8.0-9.5
	Ni	Nb	V	Al	N	Mo
	max 0.40	0.06-0.10	0.18-0.25	max 0.04	0.03-0.07	0.85-1.05

Table 1: Mean composition of X10CrMoVNb9-1 steel

The austenitization of the base material corresponds to the martensite to austenite transformation i.e. to a bcc $\rightarrow$ fcc phase change that can be identified from dilatometry tests -generally performed at different constant heating rates-. The evolution of the austenite fraction y(T) as identified from such dilatometry tests is given in figure 1. The tempered martensite to austenite transformation at equilibrium -i.e. at an infinitely slow heating rate- can be extrapolated from these curves. It has been proposed in Duthilleul and Brachet (2005) that the transformation kinetics close to equilibrium can be modelled by a Jonhson-Mehl-Avrami law:

$$y_{eq} = 1 - \exp(-(K_0(T - A_{eq0}))^{m_0}) \tag{4}$$

The approach that is proposed herein to model austenitization during heating at higher temperature rates is based on the assumption that the transformation can be splitted into two successive steps, viz. first, an incubation stage and then an initiation-and-growth stage. As proposed by different authors, after discretization of the heating process in a set of isothermal steps Δt at temperature T_i, the incubation time during any anisothermal heating T(t) -for instance at a constant heating rate-, can be related to the incubation times $t_i(T_i)$ during isothermal transformation at temperatures T_i, by using a Scheil additivity principle (6). Besides, it has been proposed in (Roux *et al.* (2006)) to model the incubation times $t_i(T_i)$ with the following phenomenological relationship:

$$t_i(T_i) = A(A_{ssat} - T_i) \exp\left(\frac{C}{T_i - A_{eq0}}\right) \tag{5}$$

$$\sum_i \frac{\Delta t_i}{t_i(T_i)} = 1 \tag{6}$$

Last, it has been proposed in (Brachet *et al.* (1998)) to model the transformation kinetics far from equilibrium with the following model:

$$\dot{y} = K \exp\left(\frac{-W}{RT}\right) \langle T(y_{eq}) - A_{eq0} \rangle_+^n (1 - y) \tag{7}$$

After identification, this model allows to describe the austenitization kinetics during any anisothermal heating loading, for instance at constant heating rates as illustrated by Fig.1 Austenite to martensite transformation during cooling can be modelled by Koistinen-Marburger model that relates martensite fraction to the difference between current temperature and so-called Martensite start temperature that is mainly material composition dependent.

These metallurgical transformations models have been implemented in Cast3M©finite element code so that fully coupled thermo-metallurgical simulations can be run -with a staggered iterative approach-.

2.3 Mechanical analyses

As already proposed herein for heat transfer analyses, depending on its current microstructure X10CrMoVNb9-1 steel can be considered as a mono- or multiphase material. The thermo-

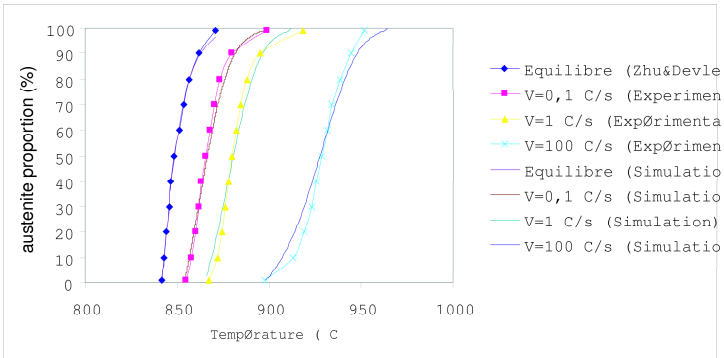

Figure 1: Austenite transformation kinetics (model and experimental results)

mechanical behaviour of each phase can be characterized from ad hoc experiments.

2.3.1 mechanical behaviour for each phase

The thermo-mechanical behaviour of each phase has been modelled within the standard internal variables formalism (Lemaître and Chaboche (1988)). Considering the temperature range to be accounted for, a standard elasto-viscoplastic Chaboche type model (Chaboche (1977)) has been chosen.

First, total strain $\underline{\underline{\varepsilon}}^t$ partition is assumed so that:

$$\underline{\underline{\varepsilon}}^t = \underline{\underline{\varepsilon}}^e + \underline{\underline{\varepsilon}}^{vp} \tag{8}$$

where $\underline{\underline{\varepsilon}}^e$ and $\underline{\underline{\varepsilon}}^{vp}$ respectively denote the thermo-elastic and viscoplastic strains.

The thermodynamical potential -chosen as the Gibbs free energy- is writen as:

$$\psi = \psi^{th-e} + \psi^{vp} \tag{9}$$

where ψ^{th-e} and ψ^{vp} respectively denote the thermo-elastic and the hardening parts.

$$\psi^{th-e} = \frac{1}{2}\underline{\underline{\varepsilon}}^e : \underline{\underline{\underline{\underline{C}}}}(T) : \underline{\underline{\varepsilon}}^e + \underline{\underline{\underline{B}}}(T) : \underline{\underline{\varepsilon}}^e + \frac{C_p(T)}{2T_o}.[T - T_0]^2 \tag{10}$$

where T denotes the current temperature. Considering an isotropic hardening mechanisms with a quadratic contribution to the free energy and two kinematic hardening mechanisms, the hardening part of the state potential is chosen as:

$$\psi^{vp} = \frac{1}{2}R_\infty(T)br^2 + \sum_{i=1}^{2}\frac{1}{2}C_i(T)\underline{\underline{\alpha}}_i : \underline{\underline{\alpha}}_i \tag{11}$$

where r and $\underline{\underline{\alpha}}_i$ (i=1, 2) respectively denote the isotropic and kinematic hardening variables. Plastic strain evolution law is derived from a potential that has been chosen as:

$$(\phi^*)^{vp} = \frac{K(T)\dot{\varepsilon}_0}{2}\beta\left[\frac{1+N}{2}; -\frac{N}{2}; \left(\tanh\left\langle\frac{f_p}{K}\right\rangle\right)^2\right] \tag{12}$$

where β denotes the incomplete Beta function and where f_p denotes the elastic domain function that is equal to $J_2(\underline{\underline{\sigma}} - \underline{\underline{X}}_i) - R - \sigma_y$. Hardening variables evolution laws are derived from a

potential $F_p(\underline{\underline{\sigma}}(T), T, \underline{\underline{X}}_i, R$ that is equal to f_p plus he following extra terms:

$$f_R = \frac{1}{2}\frac{R^2}{R_\infty} \quad ; \quad f_{\underline{\underline{X}}_1} = \frac{1}{2}\frac{\gamma_1(T)}{C_1(T)}\underline{\underline{X}}_1 : \underline{\underline{X}}_1 \quad ; \quad f_{\underline{\underline{X}}_2} = 0 \tag{13}$$

Normality rule give:

$$\dot{\underline{\underline{\varepsilon}}}^p = \frac{3}{2}\dot{\lambda}\frac{s\left[\underline{\underline{\sigma}} - \underline{\underline{X}}_i\right]}{J_2\left[\underline{\underline{\sigma}} - \underline{\underline{X}}_i\right]} \tag{14}$$

With state laws, we have:

$$\dot{\underline{\underline{\sigma}}} = \underline{\underline{\underline{\underline{E}}}}(T)\,\dot{\underline{\underline{\varepsilon}}}^e + \frac{\partial \underline{\underline{\underline{\underline{E}}}}}{\partial T}(T)\,\dot{\underline{\underline{\varepsilon}}}^e\,\dot{T} - \frac{E(T)}{1-2\nu}(T-T_0)\,\dot{T}\,\underline{\underline{I}}\left[\frac{\alpha(T)}{T-T_0} + \frac{\partial \alpha}{\partial T} + 2\alpha(T)\frac{\frac{\partial \nu}{\partial T}}{1-2\nu} - \alpha(T)\frac{\frac{\partial E}{\partial T}}{E}\right] \tag{15}$$

$$\dot{R} = b(T)\,\dot{\lambda}\left[R_\infty(T) - R\right] + \dot{T}\,R\left[\frac{\frac{dR_\infty}{dT}}{R_\infty(T)} - \frac{\frac{db}{dT}}{b(T)}\right] \tag{16}$$

$$\dot{\underline{\underline{X}}}_1 = C_1(T)\dot{\underline{\underline{\varepsilon}}}^p - \gamma_1(T)\,\dot{\lambda}\,\underline{\underline{X}}_1 + \frac{\frac{dC_1}{dT}}{C_1(T)}\underline{\underline{X}}_1.\dot{T} \tag{17}$$

$$\dot{\underline{\underline{X}}}_2 = C_2(T)\dot{\underline{\underline{\varepsilon}}}^p + \frac{\frac{dC_2}{dT}}{C_2(T)}\underline{\underline{X}}_1.\dot{T} \tag{18}$$

where $\dot{\lambda} = \frac{\partial(\phi^*)^{vp}}{\partial f_p} = \dot{\varepsilon}_0\left[\sinh\left\langle\frac{f_p}{K}\right\rangle\right]^N = \dot{p} = \sqrt{\frac{2}{3}\dot{\underline{\underline{\varepsilon}}}^p : \dot{\underline{\underline{\varepsilon}}}^p}$ denotes the cumulated plastic strain.

This model has been identified from room temperature to 800°C for the tempered martensite phase, from 400 to 1200°C for the austenite phase and from 300°C to room temperature for the martensite phase.

2.3.2 Thermo-mechanical behaviour during a phase transformation

Different approaches have been proposed to model the mechanical behaviour of materials during a phase transformation (see for instance Leblond *et al.* (1986)), Hamata (1991) or Coret (2002). Herein, it is proposed to assume that the state of the material can be modelled by a state potential that is a built from the state potential of each phase and a simple mixture law. Furthermore, so-called transformation plasticity mechanism must be taken into account as well as the so-called inheritage of hardening from the mother phase to the daughter phase. It can be shown that residual stresses prediction are sensitive to both phenomena.

3 Conclusions

Simple GTA welding tests have been developed (Roux *et al.* (2006)) in order to validate the numerical tool that is developed. The following figures give illustration of the microstructure field that could be predicted and compared to experimental evidences for a so-called Disk-spot GTA welding test. This model has also been used to simulate Satoh experiments that corresponds to thermal cyclic loading applied to specimens at constant total strain.

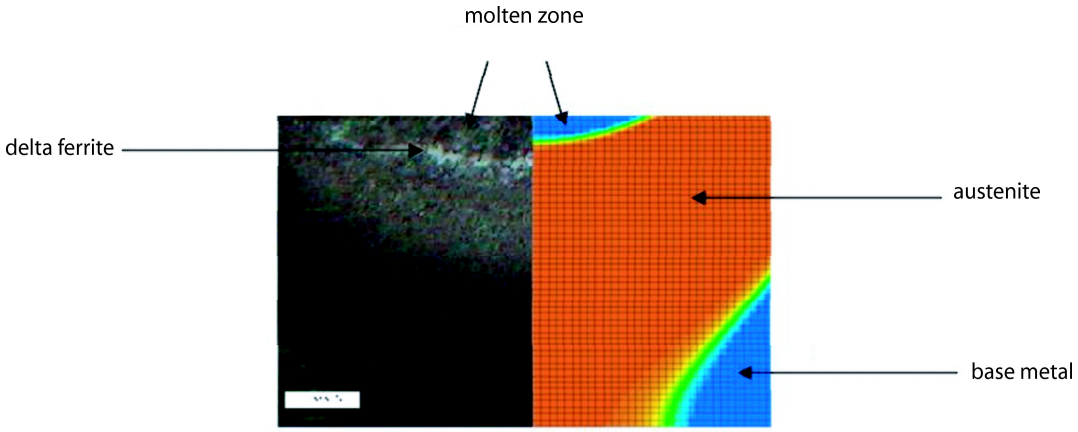

Figure 2: microstructure obtained at the end of the heating during a Disk-spot GTA welding test

References

Duthilleul, R., Brachet, J.-C. 1993 Etude des évolutions microstructrales lors d'un traitement thermique rapide à haute température d'un acier de type T91 *Document technique CEA/DMN* 248, 513-520

Brachet, J.-C., Gavard, L., Boussidan, C., Lepoittevin, C., Denis, S., Servant, C. 1998 Modelling of Phase Transformations Occuring in Low Activation Martensitic Steels *J. of Nuclear Materials* 258-263, 1998, pp 1307-1311

Leblond, J.-B., Mottet, G., Devaux, J.-C. 1998 A theorical and numerical approach to the plastic behaviour of steels during phase transformations-I Derivation of general relations *J. Mech. Phys. Solids* 34, 1986, pp 395-409

Hamata, N., Billardon, R., Marquis, D., Ben Cheickh, A. 1991 A model for nodular graphite cast iron coupling anisothermal elasto-viscoplasticity and phase transformation *Constitutive laws for engineering materials, ASME Press, Desai CS et aL. editors* pp 593-596

Coret, M., Combescure, A. 2002 A mesomodel for the numerical simulation of the multiphasic behaviour of materials under anisothermal loading *Int. J. of Machanical Sciences* 44, 2002,pp 1947-1963

Roux, G.M., Hild, F., Billardon, R. 2002 Modélisation de la transformation austénitique au chauffage d'un acier martensitique *Colloque MECAMAT* Aussois, 2006

Roux, G.M., Billardon, R. 2006 Identification of thermal boundary conditions and thermo-metallurgical behaviour of X10CrMoVNb9-1 steel *8th Int. Seminar "Numerical Analysis of Weldability"* La Defense, 2006

Roux, G.M., Billardon, R. 2006 Study of residual stresses induced by a TIG welding operation *Congrès SNS* La Defense, 2006

Lemaitre, J., Chaboche, J.-L. 1988 Mécanique des matériaux solides *Dunod 2nd, 1988*

Chaboche, J.-L. 1977 Sur l'utilisation des variables d'état internes pour la description du comportement viscoplastique et de la rupture par endommagement *Symposium franco-polonais, Problèmes non linéaires de Mécanique* Cracovie, 1977